FULL-WAVE LOSS ANALYSIS OF NORMAL- AND SUPERCONDUCTING TRANSMISSION LINES BY HYBRID-MODE BOUNDARY INTEGRAL EQUATION METHOD

W. Schroeder, Member, IEEE and I. Wolff, Fellow, IEEE

Department of Electrical Engineering and Sonderforschungsbereich 254
Duisburg University, Bismarckstr. 69, D-4100 Duisburg 1, FRG

ABSTRACT

The Hybrid-Mode Boundary Integral Equation Method is extended to full-wave analysis of arbitrary MMIC transmission lines that incorporate superconductors and/or normal (imperfect) conductors and lossy dielectrics. The method is demonstrated for thin film microstrip line of small width. Attenuation and effective permittivity results of several configurations with Au and YBCO strips separated by medium and high permittivity films are compared.

INTRODUCTION

Continued reduction of conductor cross-sections in MMIC transmission lines has made conductor losses a problem which deserves increased attention. This applies to

(i) accurate modeling of transmission lines as due to existing technology with conventional conductors, and
(ii) evaluation of low loss alternatives with high-T_c superconductors.

It is important to note that imperfect conductors do not only add to transmission line loss, but may considerably affect phase velocity and alter the dispersion characteristic for cross-sectional dimensions that are not large compared to the skin depth or the penetration depth, respectively, in the superconducting case. The concept that by continued reduction of dimensions the quasi-static regime will ultimately be reached is correct only for perfect conductors. For real conductors and dimensions comparable to the skin or penetration depth there is poor accuracy with approximate loss calculations which are based on the static field distributions. Full wave analysis is required in this case.

Full-wave loss analyses for *finite thickness* (normal) conductors have been reported using e.g. the Finite-Element Method [1], the Method of Lines [2] and the Mode-Matching Method [3]. For high conductivity materials this kind of analysis is numerically demanding because of the large ratio $\sigma/\omega\varepsilon_0$ and difficulties to represent accurately the almost vanishing fields within the conductors. It may be expected to be even more demanding for superconducting transmission lines. Analysis of superconducting structures up to now was in fact either by means of approximate models like [4] or restricted to layered configurations of infinite extent or zero thickness [5-7].

This paper demonstrates the application of the Hybrid-Mode Boundary Integral Equation Method [8] to the analysis of general transmission lines with normal conductors, superconductors and lossy dielectrics. Advantages of this approach are its *flexibility* to cope with arbitrary shielded or unshielded transmission line cross-sections and its *reliability* in that the origin of spurious solutions, still a major problem in finite-element, finite difference and spectral domain approaches, has been eliminated [9].

METHOD OVERVIEW

The field theoretic method is an extension of the space domain hybrid-mode boundary integral equation method the principle of which was described in [8]. Given an arbitrary structure which is translationally invariant with respect to the axial unit vector $\boldsymbol{a}$, we interest for solutions that vary with time and axial coordinate like $\exp(j\omega t - \gamma \boldsymbol{a}\boldsymbol{r})$ where $\gamma \in \mathbb{C}$. Suppressing the common factor we look at the electric and magnetic field as functions $\boldsymbol{E},\boldsymbol{H}: \mathbb{R}^2 \to \mathbb{C}^3$ of transversal coordinates only. The basic idea of the boundary integral approach now is, that $\boldsymbol{E}$ and $\boldsymbol{H}$ in the interior of a homogeneously filled subregion $\Omega \subset \mathbb{R}^2$ of the transverval plane are uniquely specified by their boundary values. Hence the problem can be formulated exclusively in terms of the axial and tangential field components $\boldsymbol{a}\cdot\boldsymbol{H}$, $\boldsymbol{t}\cdot\boldsymbol{E}$, $\boldsymbol{a}\cdot\boldsymbol{E}$, $\boldsymbol{t}\cdot\boldsymbol{H}: \partial\Omega \to \mathbb{C}$ along the subregion boundaries (Fig.1). This approach circumvents any numerical problems associated with the discretization of almost vanishing fields in subregions of good or superconducting media. The dispersive properties of the medium in subregion Ω are described by the two functions

$$z : \mathbb{R} \to \mathbb{C},\ \omega \mapsto j\omega\mu_0(\mu_r'(\omega) - j\mu_r''(\omega)) \quad (1a)$$

and

$$y : \mathbb{R} \to \mathbb{C},\ \omega \mapsto \sigma'(\omega) - j\sigma''(\omega) + j\omega\varepsilon_0(\varepsilon_r'(\omega) - j\varepsilon_r''(\omega)). \quad (1b)$$

CH2870-4/91/0000-0341$01.00 © 1991 IEEE

There are no restrictions on the medium apart from being linear and isotropic. Hence this description complies well with linear models of superconductivity. Such models reduce to a temperature and frequency dependent conductivity as does for instance the well known two fluid model

$$\sigma(T,\omega) = \sigma_{nc}\left(\frac{T}{T_c}\right)^4 - j\,\frac{1}{\omega\mu_0\,\lambda(0)^2}\left(1-\left(\frac{T}{T_c}\right)^4\right) \qquad (2)$$

where σ_{nc} denotes the normal state conductivity just above the critical temperature T_c and $\lambda(0)$ denotes penetration depth at $T=0$.

The fields within Ω being uniquely specified by the four boundary value functions $\boldsymbol{a}\cdot\boldsymbol{H}$, $\boldsymbol{t}\cdot\boldsymbol{E}$, $\boldsymbol{a}\cdot\boldsymbol{E}$, $\boldsymbol{t}\cdot\boldsymbol{H}: \partial\Omega \to \mathbb{C}$ we have to establish a set of equations to determine the latter. In the absence of interior sources, it follows from Maxwells equations, that the axial components $\boldsymbol{a}\cdot\boldsymbol{H}$ and $\boldsymbol{a}\cdot\boldsymbol{E}$ are solutions of the homogeneous Helmholtz equation

$$\Delta u + \left(\gamma^2 - z(\omega)y(\omega)\right)u = 0. \qquad (3)$$

Solutions of (3) can be found as solutions of the associated boundary integral equation. To introduce the latter we need a few definitions. Let $Q \subset \mathbb{C}$ denote the union of the negative imaginary halfplane and the positive real axis and take

$$h(\omega,\gamma) = \sqrt{\gamma^2 - z(\omega)y(\omega)} \quad \in Q \qquad (4)$$

with z and y given by eqns. (1). As a fundamental solution of the 2-D Helmholtz equation (3) appropriate for subregion Ω we may then introduce the function

$$g(\boldsymbol{p},\boldsymbol{q}): \Omega\times\Omega \setminus \mathrm{Diag}(\Omega\times\Omega) \to \mathbb{C},\ (\boldsymbol{p},\boldsymbol{q}) \mapsto K_0(jh\|\boldsymbol{p}-\boldsymbol{q}\|) \qquad (5)$$

where K_0 is the modified Bessel function of the second kind and zero order. This fundamental solution well defined for arbitrary complex media as described by eqns. (1). Solutions of (3) may now be obtained from the boundary integral operator equation

$$\mathbf{K}[u] - \mathbf{G}\left[\frac{\partial u}{\partial \boldsymbol{n}}\right] = 0, \qquad (6)$$

with the operators given by

$$\mathbf{G}[v](\boldsymbol{p}) := \int_{\partial\Omega\setminus\{\boldsymbol{p}\}} g(\boldsymbol{p},\boldsymbol{q})\,v(\boldsymbol{q})\,ds(\boldsymbol{q}) \qquad (7)$$

$$\mathbf{K}[u](\boldsymbol{p}) := \int_{\partial\Omega\setminus\{\boldsymbol{p}\}} \mathrm{grad}_q\, g(\boldsymbol{p},\boldsymbol{q})\,u(\boldsymbol{q})\,ds(\boldsymbol{q}). \qquad (8)$$

A definition of $\mathbf{K}$ in terms of uniformly convergent boundary integrals was given in [8]. Upon the proper substitutions from Maxwells equations the following integral equation system for the boundary values on $\partial\Omega$ is obtained

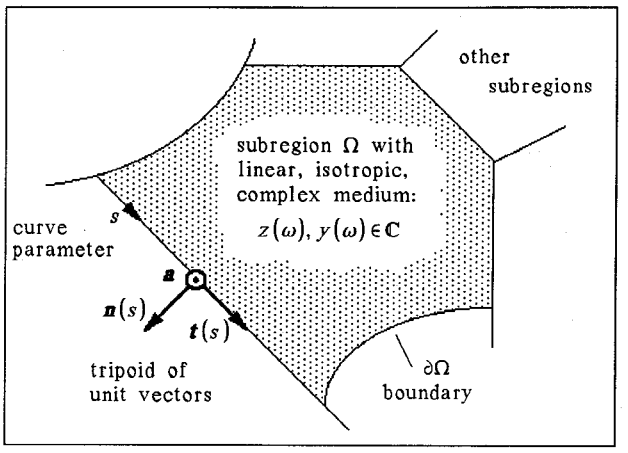

Fig.1: Definitions relative to a homogeneous subregion Ω of the transmission line cross-section.

$$\mathbf{K}[\boldsymbol{a}\boldsymbol{H}] - \frac{h^2}{z}\mathbf{G}[\boldsymbol{t}\boldsymbol{E}] - \frac{\gamma}{z}\mathbf{G}\left[\frac{\partial}{\partial s}\boldsymbol{a}\boldsymbol{E}\right] = 0, \qquad (9a)$$

$$\mathbf{K}[\boldsymbol{a}\boldsymbol{E}] + \frac{h^2}{y}\mathbf{G}[\boldsymbol{t}\boldsymbol{H}] + \frac{\gamma}{y}\mathbf{G}\left[\frac{\partial}{\partial s}\boldsymbol{a}\boldsymbol{H}\right] = 0\ . \qquad (9b)$$

The unkown boundary value functions in (9) always belong to two subregions thereby satisfying continuity requirements. B-splines are used for their discretization. For the overall structure a homogeneous system of integral equations emerges which is solved numerically by the *method of least squares with intermediate projection* [9]. As opposed to the *Galerkin* and other *method of moments* approaches which introduce *spurious solutions* in Boundary-Element, Finite-Element, Finite Difference and Spectral Domain Approaches for electromagnetic field eigenvalue problems, this method provides a reliable discretization. The present analysis demonstrates absence of spurious modes for non-trivial problems.

APPLICATION TO THIN FILM MICROSTRIP LINE

The use of thin-film microstrip (TFMS) line with conventional conductors has been reported e.g in [10]. Apart from its low chip size requirements it has the advantage to combine well with active devices because both strip and ground conductor are accessible from the top side of the substrate. The drawback of conventional TFMS line is its high attenuation. With the advent of the new high-T_c materials however TFMS may become an interesting alternative to coplanar waveguide in MMIC applications [4]. We have performed full-wave analysis to obtain propagation constant and attenuation for several TFMS configurations with Au and YBCO conductors and different film and substrate materials. The simplified model of

Fig.2 has the ground conductor replaced by an infinite perfectly conducting plane. The effect of finite ground metalization and substrate becomes obvious by comparing results with that for the more realistic model of Fig.3. Effective permittivities $\varepsilon_{eff} := (\beta/k_0)^2$ are given in Fig.4 for the case of Si_3N_4 films ($\varepsilon_r' = 7.3$) and in Fig.5 for $LaAlO_3$ film ($\varepsilon_r' = 24.5$). The corresponding transmission line losses are given in Fig.6 for Au conductors with $\sigma' = 4.3\times10^7\,(\Omega m)^{-1}$ and in Fig.7 for $YBa_2Cu_3O_{7-x}$ at 77K. The latter was modeled in accordance with eqn.(2) by

$$\sigma(f) = (4\cdot10^6 - j\,\frac{2\cdot10^9}{f/GHz})(\Omega m)^{-1} \quad \text{for } T = 77K \qquad (10)$$

corresponding to $\lambda(77K) = 260nm$ after measurements reported in [11]. The different curves labeled 1-13 relate to different combinations of substrate material, conductor material and strip thickness t as listed in Table I. GaAs ($\varepsilon_r' = 12.9$) was assumed for the substrate in Fig.3. Dielectric losses were ignored everywhere but in configuration 13.

For all examples a considerable increase of effective permittivity is observed for Au and YBCO strips against perfectly conducting strips. The increase can be understood as due to the contributions of internal inductance L_i' (in the case of normal conductors) and kinetic inductance L_k' (for superconductors) which add to the geometric inductance L_g'. If we accept a parallel plate waveguide with conductor separation d as an approximate model their contributions can be estimated by

$$\frac{\varepsilon_{eff,normal\ cond.}}{\varepsilon_{eff,perfect\ cond.}} \approx 1 + \frac{L_i'}{L_g'} \approx 1 + \frac{\delta}{d} \qquad (11)$$

$$\frac{\varepsilon_{eff,superconductor}}{\varepsilon_{eff,perfect\ cond.}} \approx 1 + \frac{L_k'}{L_g'} \approx 1 + \frac{\lambda}{d} \qquad (12)$$

provided that t is much larger than skin depth δ and penetration depth λ. While λ is independent of frequency, δ behaves like the inverse square root of frequency. Hence (11) and (12) are in principal agreement with the full-wave results of Figs.4-7. Better approximations are found e.g. in [5]. On an expanded scale a small decrease of effective permittivity over frequency is observed for the superconducting examples.

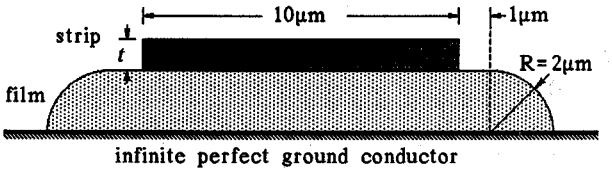

Fig.2: Simplified model of thin film microstrip line.

CONCLUSION

The space-domain hybrid mode boundary integral equation method is extended to the analysis of waveguide with arbitrary complex media. The approach has some distinct advantages with respect to analysis of good conductors and superconductors. Fields within conductors are represented exclusively by their boundary values. Hence numerical problems due to discretization of eventually very small interior fields can not arise. Furthermore the problem of sensitivity to discretization [2] is significantly reduced. As opposed to [3] the method allows for arbitrary conductor shape including curved boundaries. Shielding is not required.

REFERENCES

[1] K. Hayata, K. Miura and M. Koshiba, "Finite-element formulation for lossy waveguides," IEEE Trans. Microwave Theory Tech., vol. 36, pp 268-276, Feb. 1988.

[2] F. J. Schmückle and R. Pregla, "The method of lines for the analysis of lossy planar waveguides," IEEE Trans. Microwave Theory Tech., vol. 38, pp. 1473-1479, Oct. 1990.

[3] W. Heinrich, "Full-wave analysis of conductor losses on MMIC transmission lines," IEEE Trans. Microwave Theory Tech., vol. 38, pp. 1468-1472, Oct. 1990.

[4] E. B. Ekholm and S. W. McKnight, "Attenuation and Dispersion for high-T_c superconducting microstrip lines," IEEE Trans. Microwave Theory Tech., vol. 38, pp. 387-395, Apr. 1990.

[5] J. M. Pond, C. M. Krowne and W. L. Carter, "On the application of complex resistive boundary conditions to model transmission lines consisting of very thin superconductors," IEEE Trans. Microwave Theory Tech., vol. 37, pp. 181-190, Jan. 1990.

[6] J. M. Pond and P. Weaver "Field and energy-density profiles in layered superconductor-dielectric structures," IEEE MTT-S 1990 Intern. Microwave Symposium Digest, pp. 277-288, Dallas, 1990.

[7] K. Araki, "Coupling characteristics of superconducting transmission lines," 3rd Asia-Pacific Microwave Conference Proceedings, Tokyo, 1990.

Fig.3: Thin film microstrip line with finite ground conductor on dielectric substrate.

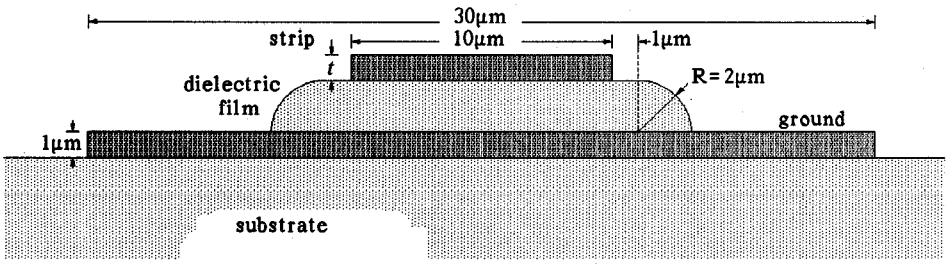

TABLE I: TFMS CONFIGURATIONS ANALYZED IN THIS PAPER
Numbers 1-13 correspond to the curves of Figs.4-7.

configuration		#1	#2	#3	#4	#5	#6	#7	#8	#9	#10	#11	#12	#13
geometry		Fig.2						Fig.3			Fig.2			
strip	$t/\mu m$	0.5			1.0			1.0						
	conductor	Au	YBCO	perf.	Au	YBCO	perf.	Au	YBCO	perf.	Au	YBCO	perf.	YBCO
film	ε_r	7.3									24.5			
	$\tan\delta$	0												10^{-4}
ground conductor		perfect						Au	YBCO	perf.	perfect			
substrate	ε_r	——						12.9			——			

Fig.4: Effective Permittivity for Si_3N_4-film

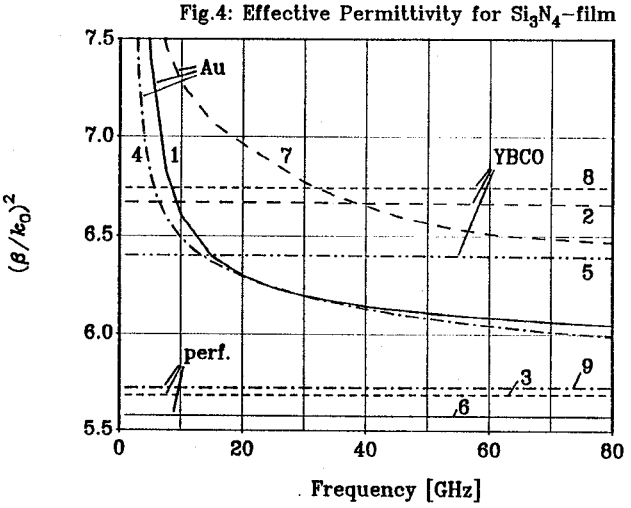

Fig.5: Effective Permittivity for $LaAlO_3$-film

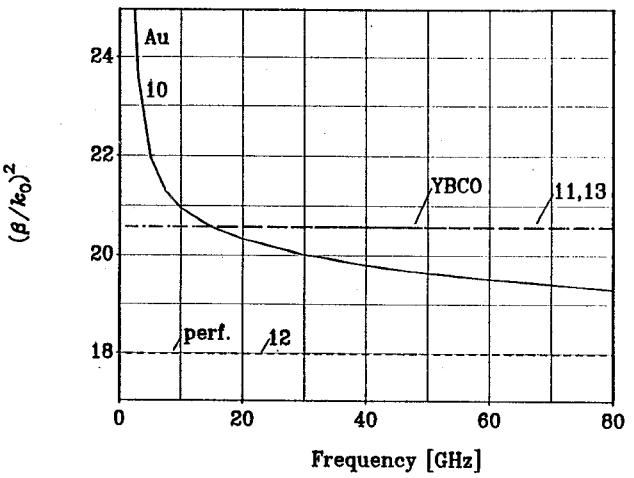

Fig.6: Attenuation for Au-conductors

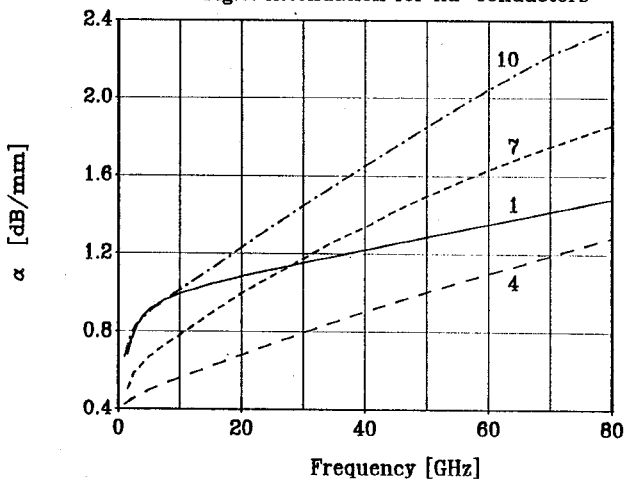

Fig.7: Attenuation for YBCO-conductors

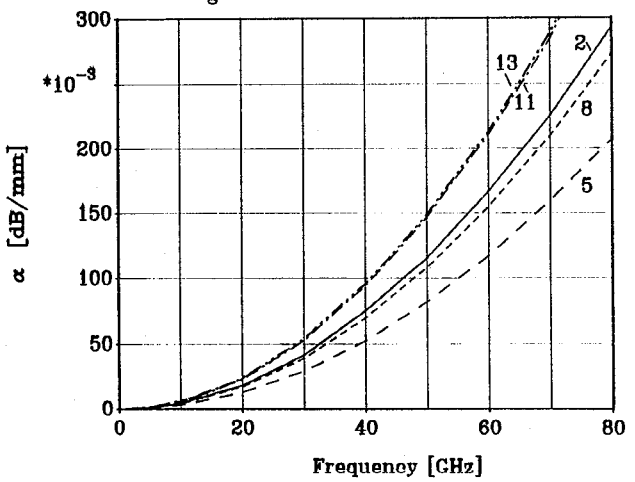

[8] W. Schroeder and I. Wolff, "A new hybrid mode boundary integral method for analysis of MMIC waveguides with complicated cross-section," IEEE MTT-S 1989 Intern. Microwave Symposium Digest, Long Beach, pp. 711-714, Jun. 1989.

[9] W. Schroeder and I. Wolff, "Full wave boundary integral analysis of arbitrary integrated transmission lines: Origin and avoidance of spurious solutions," Proceedings of the 20th European Microwave Conference, Budapest, Sep. 1990.

[10] T. Hiraoka, T. Tokumitsu, M. Aikawa, "Very small wide-band MMIC magic T's using microstrip lines on a thin dielectric film," IEEE Trans. Microwave Theory Tech., vol. 37, pp. 1569-1575, Oct. 1989.

[11] H. Chaloupka, N. Klein, S. Orbach, "Effect of finite thickness on the surface impedance of hight-T_c thin films," IEEE MTT-S 1990 Intern. Microwave Symposium Digest, pp. 855-858, Dallas, 1990.